Inorg. Chem. **2006**, *45*, 147–155

Phosphorescent Cu(I) Complexes of 2-(2′-pyridylbenzimidazolyl)benzene: Impact of Phosphine Ancillary Ligands on Electronic and Photophysical Properties of the Cu(I) Complexes

Theresa McCormick, Wen-Li Jia, and Suning Wang*

Department of Chemistry, Queen's University, Kingston, Ontario, K7L 3N6 Canada

Received August 18, 2005

Four mononuclear Cu(I) complexes of 2-(2′-pyridyl)benzimidazolylbenzene (pbb) with four different ancillary phosphine ligands PPh_3, bis[2-(diphenylphosphino)phenyl]ether (DPEphos), bis(diphenylphosphino)ethane (dppe), and bis-(diphenylphosphinomethyl)diphenylborate (DPPMB) have been synthesized. The crystal structures of [Cu(pbb)-$(PPh_3)_2$][BF_4] (1), [Cu(pbb)(dppe)][BF_4] (**2**), [Cu(pbb)(DPEphos)][BF_4] (**3**), and the neutral complex [Cu(pbb)(DPPMB)] (**4**) were determined by single-crystal X-ray diffraction analyses. The impact of the phosphine ligands on the structures of the copper(I) complexes was examined, revealing that the most significant impact of the phosphine ligands is on the P–Cu–P bond angle. The electronic and photophysical properties of the new complexes were examined by using UV–vis, fluorescence, and phosphorescence spectroscopies and electrochemical analysis. All four complexes display a weak MLCT absorption band that varies considerably with the phosphine ligand. At ambient temperature, no emission was observed for any of the complexes in solution. However, when doped into PMMA polymer (20 wt %), at ambient temperature, all four complexes emit light with a color ranging from green to red-orange, depending on the phosphine ligand. The emission of the new copper complexes has an exceptionally long decay lifetime (>200 μs). Ab initio MO calculations established that the lowest electronic transition in the copper(I) complexes is MLCT in nature. The electronic and photophysical properties of the new mononuclear Cu(I) complexes were compared with those of the corresponding polynuclear Cu(I) complexes based on the 2-(2′-dipyridyl)benzimidazolyl derivative ligands and the previously extensively studied phenanthroline-based Cu(I) complexes.

Introduction

Extensive research efforts have been centered on phosphorescent Cu(I) complexes based on phenanthroline and its derivative ligands because of their potential applications in photochemistry and organic light-emitting diodes.[1−3] In addition, many luminescent Cu(I) complexes based on polypyridyl chelate ligands have also been investigated.[2] Recently, our group initiated the investigation of phosphorescent Cu(I) complexes based on the 2-(2′-pyridyl)benzimidazolyl chelating unit.[4] We reported a group of room-temperature phosphorescent polynuclear Cu(I) complexes, their photophysical properties, and their applications in organic light-emitting diodes (OLEDs).[4] This group of polynuclear Cu(I) complexes is based on linear or star-shaped ligands that contain two or more of the 2-(2′-pyridyl)-benzimidazolyl chelating units linked together by an aromatic group such as benzene or biphenyl. The coordination sphere of the Cu(I) center in this group of complexes is completed by two ancillary PPh_3 ligands, an example of which,

* To whom correspondence should be addressed. E-mail: wangs@chem.queensu.ca.

(1) (a) Cuttell, D. G.; Kuang, S. M.; Fanwick, P. E.; McMillin, D. R.; Walton, R. A. *J. Am. Chem. Soc.* **2002**, *124*, 6. (b) Kuang, S. M. Cuttell, D. G.; McMillin, D. R.; Fanwick, P. E.; Walton, R. A. *Inorg. Chem.* **2002**, *41*, 3313.

(2) (a) Yao, Y.; Perkovic, M. W.; Rillema, D. P.; Woods, C. *Inorg. Chem.* **1992**, *31*, 3956. (b) Armaroli, N.; Balzani, V.; Barigelletti, F.; De Cola, L.; Flamigni, L.; Sauvage, J. P.; Hemmert, C. *J. Am. Chem. Soc.* **1994**, *116*, 5211. (c) Dietrich-Buchecker, C. O.; Nierengarten, J. F.; Sauvage, J. P.; Armaroli, N.; Balzani, V.; De Cola, L. *J. Am. Chem. Soc.* **1993**, *115*, 11237. (d) Yam, V. W. W.; Lo, K. K. W. *J. Chem. Soc., Dalton Trans.* **1995**, 499. (e) Juris, A. Ziessel, R. *Inorg. Chim. Acta* **1994**, *225*, 251. (f) Youinou, M. T.; Ziessel, R.; Lehn, J. M. *Inorg. Chem.* **1991**, *30*, 2144. (g) Balzani, V.; Juris, A.; Venturi, M. *Chem. Rev.* **1996**, *96*, 759 and references therein.

(3) Zhang, Q.; Zhou, Q.; Cheng, Y.; Wang, L.; Ma, D.; Jing, X.; Wang, F. *Adv. Mater.* **2004**, *16*, 432.

(4) Jia, W. L.; McCormick, T.; Tao, Y.; Lu, J. P.; Wang, S. *Inorg. Chem.* **2005**, *44*, 5706.

10.1021/ic051412h CCC: $33.50
Published on Web 12/03/2005

Chart 1. Structure of $[Cu_2(bmbp)(PPh_3)_4]^{2+}$

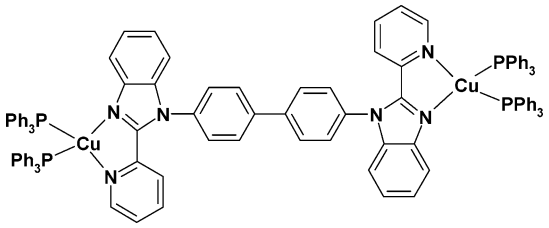

Chart 2. General Structure of $[Cu_2(pbb)(P)_2]^{+/0}$

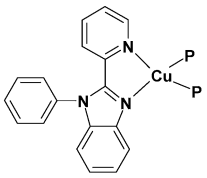

The general structure of $[Cu_2(pbb)(P)_2]^{+/0}$

(P)$_2$: $(PPh_3)_2$, (**1**), dppe, (**2**)

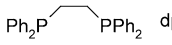

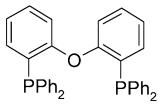

DPEphos, (**3**)

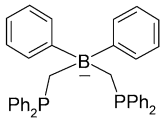

DPPMB, (**4**)

$[Cu_2(bmbp)(PPh_3)_4][BF_4]_2$, is shown in Chart 1. Our investigation established that the phosphorescence of this group of complexes originates from a metal−ligand charge-transfer (MLCT) transition with a remarkably long decay lifetime involving the Cu(I) center and the 2-(2′-pyridyl)benzimidazolyl chelating unit.[4] Preliminary evaluation results indicated that these polynuclear Cu(I) complexes can be used as emitters in OLEDs; however, the device efficiency is low.[4] As noted by McMillin and co-workers for phosphorescent Cu(I) complexes based on a phenanthroline *N*,*N*-chelate (or its derivative), the ancillary phosphine donors, albeit not involved in the MLCT transition, play a key role in stabilizing the Cu(I) center and have a significant impact on the photophysical properties of the complex.[1] Further evidence for the role of the phosphine ligands came from a recent report by L. X. Wang and co-workers where they noted that the performance of $[Cu(Phen)(DPEphos)][BF_4]$ in OLEDs {DPEphos = bis[2-(diphenylphosphino)phenyl]-ether, phen = 1,10-phenanthroline and derivatives} is much better than that of $[Cu(Phen)(PPh_3)_2][BF_4]$, because of the increased emission quantum efficiency and the shortened decay lifetime.[3] Clearly, the appropriate choice of the ancillary phosphine ligands is very important in optimizing the performance of the Cu(I) complexes. Although both phenanthroline and 2-(2′-pyridyl)benzimidazolyl are *N*,*N*-chelate ligands, they have distinct geometric and electronic properties. As a result, the effects of the ancillary phosphine ligands on the properties of the corresponding Cu(I) complexes are not necessarily the same. Therefore, to establish the effects of the phosphine ligands on the properties 2-(2′-pyridyl)benzimidazolyl-based Cu(I) complexes, and hence to find a better phosphorescent Cu(I) emitter for OLEDs, it is necessary to examine the structures and photophysical properties of a series of Cu(I) 2-(2′-pyridyl)benzimidazolyl complexes involving different phosphine ancillary ligands, which is the focus of this report. To simplify our investigation, we focused on a group of mononuclear Cu(I) complexes containing the 2-(2′-pyridyl)benzimidazolylbenzene (pbb) ligand with the common structure of $[Cu(pbb)(P)_2]^{+/0}$, as shown in Chart 2. The four different phosphine ligands used in our investigation are PPh_3, bis(diphenylphosphino)ethane (dppe), bis[2-(diphenylphosphino)phenyl]ether (DPEphos), and bis(diphenylphosphinomethyl)diphenylborate (DPPMB). Herein, we report the syntheses, crystal structures, photophysical properties, and results of molecular orbital calculations of four new Cu(I) complexes that contain the common pbb chelate ligand and the four different phosphine ligands.

Experimental Section

All starting materials were purchased from Aldrich Chemical Co. and used without further purification. Solvents were freshly distilled over appropriate drying reagents under N_2 atmosphere. All experiments were carried out under a dry nitrogen atmosphere using standard Schlenk techniques unless otherwise stated. Thin layer chromatography (TLC) was carried out on silica gel. Flash chromatography was carried out on silica (silica gel 60, 70−230 mesh). ^{1}H and ^{31}P NMR spectra were recorded on a Bruker Avance 300 MHz spectrometer. Excitation and emission spectra were recorded on a Photon Technologies International QuantaMaster model C-60 spectrometer. Emission lifetimes were measured on a Photon Technologies International Phosphorescent spectrometer (Time-Master C-631F) equipped with a xenon flash lamp and digital emission photon multiplier tube using a band pathway of 5 nm for excitation and 2 nm for emission. Elemental analyses were performed by Canadian Microanalytical Service Ltd., Delta, British Columbia, Canada. Cyclic voltammetry was performed using a BAS CV-50W analyzer with a scan rate of 500 mV s^{-1}. The electrolytic cell used was a conventional three-compartment cell, in which a Pt working electrode, a Pt auxiliary electrode, and a Ag/AgCl reference electrode were employed. The CV measurements were performed at room temperature using 0.10 M tetrabutylammonium hexafluorophosphate (TBAP) as the supporting electrolyte and CH_3CN as the solvent. The ferrocenium/ferrocene couple was used as the internal standard (E_0 = 0.45 V). The copper(I) complexes[5] $[Cu(CH_3CN)_4][BF_4]$,$[Cu(CH_3CN)_2(PPh_3)_2][BF_4]$,$[Ph_2B(CH_2PPh_2)_2]$-ASN (ASN=5-azonia-spiro[4.4]nonane),[6] and DPEphos[7] were synthesized according to literature procedures.

Ab initio molecular orbital calculations were performed for complexes **1**−**4**. The geometric parameters from X-ray diffraction analysis and the Gaussian suite of programs (Gaussian 03)[8] were used for the calculations. The calculations were performed with the B3LYP/6-311++G** basis set at the RHF (restricted Hartree−Fock) level of computation. The orbital diagrams were generated using GaussView.

Synthesis of 2-(2-Pyridylbenzimidazolyl)benzene (pbb). A mixture of bromobenzene (1 mL, 4.27 mmol), 2-(2-pyridyl)-benzimidazole (0.505 g, 2.6 mmol), copper(I) iodide (77 mg, 0.40

(5) (a) Kubas, G. J. *Inorg. Synth.* **1979**, *19*, 90. (b) Diez, J.; Falagan, S.; Gamasa, P.; Gimeno, J. *Polyhedron* **1988**, *7*, 37.
(6) (a) Thomas J. C.; Peters, J. C.. *J. Am. Chem. Soc.* **2001**, *123*, 5100. (b) Thomas J. C.; Peters, J. C. *Inorg. Chem.* **2003**, *42*, 5055. (c) Thomas J. C.; Peters, J. C. *J. Am. Chem. Soc* **2003**, *125*, 8870.
(7) Kranenburg, M., van der Burgt, Y. E. M.; Kamer, P. C. J.; van Leeuwen, P. W. N. M. *Organometallics* **1995**, *14*, 3081.

Table 1. Crystallographic Data for Compounds **1**−**4**

	1	**2**	**3**	**4**
formula	$C_{54}H_{43}N_3P_2F_4BCu$	$C_{44}H_{37}N_3F_4P_2B_1Cu{\cdot}0.5CH_2Cl_2$	$C_{54}H_{41}N_3F_4OBP_2Cu$	$C_{56}H_{47}N_3BP_2Cu{\cdot}0.5C_7H_8{\cdot}CH_2Cl_2$
fw	946.2	862.52	960.18	1029.24
space group	$P2_1$	$P2_1/n$	Cc	$P\bar{1}$
a, Å	9.961(2)	15.919(4)	9.2812(16)	13.261(3)
b, Å	18.067(3)	15.664(3)	20.546(3)	22.435(5)
c, Å	13.206(3)	17.884(4)	23.425(4)	17.237(4)
β, deg	102.720(3)	109.314(4)	90.608(3)	91.299(4)
V, Å^3	2318.4(8)	4208.6(16)	4466.7(13)	5127(2)
Z	2	4	4	4
D_{calc}, g cm^{-3}	1.355	1.361	1.428	1.333
μ, cm^{-1}	5.97	7.11	6.22	6.36
$2\theta_{max}$, deg	56.28	56.76	56.40	56.52
no. of reflns measd	14005	23568	12483	28503
no. of reflns used (R_{int})	7943	9664	8138	11462
	(0.0468)	(0.0460)	(0.0220)	(0.0365)
no. of params	582	526	595	627
final R [$I > 2\sigma(I)$]	0.0538	0.0810	0.0356	0.0649
R1[a]	0.0996	0.1974	0.0770	0.1652
wR2[b]				
R (all data)				
R1[a]	0.1031	0.1649	0.0394	0.1089
wR2[b]	0.1156	0.2377	0.0780	0.1929
GOF on F^2	0.997	1.037	1.105	1.018

[a] $R1 = \sum[|F_o| - |F_c|]/\sum|F_o|$. [b] $wR2 = \{\sum[w(F_o^2 - F_c^2)]/\sum(wF_o^2)\}^{1/2}$. $w = 1/[\sigma^2(F_o^2) + (0.075P)^2]$, where $P = [\max(F_o^2,0) + 2F_c^2]/3$.

Table 2. Selected Bond Lengths (Å) and Angles (deg)

		Compound **1**	
Cu(1)−N(1)	2.091(4)	N(1)−Cu(1)−N(2)	78.62(16)
Cu(1)−N(2)	2.092(4)	N(1)−Cu(1)−P(1)	119.48(12)
Cu(1)−P(1)	2.2371(13)	N(2)−Cu(1)−P(1)	116.58(11)
Cu(1)−P(2)	2.2899(15)	N(1)−Cu(1)−P(2)	105.02(12)
		N(2)−Cu(1)−P(2)	103.20(12)
		P(3)−Cu(1)−P(2)	124.12(6)
		Compound **2**	
Cu(1)−N(2)	2.009(5)	N(2)−Cu(1)−N(1)	80.1(2)
Cu(1)−N(1)	2.123(5)	N(2)−Cu(1)−P(2)	126.69(15)
Cu(1)−P(2)	2.2538(16)	N(1)−Cu(1)−P(2)	120.98(14)
Cu(1)−P(1)	2.2586(16)	N(2)−Cu(1)−P(1)	114.71(15)
		N(1)−Cu(1)−P(1)	126.32(14)
		P(2)−Cu(1)−P(1)	92.02(6)
		Compound **3**	
Cu(1)−N(2)	2.053(2)	N(2)−Cu(1)−N(1)	78.87(9)
Cu(1)−N(1)	2.114(2)	N(2)−Cu(1)−P(2)	121.74(6)
Cu(1)−P(2)	2.2346(8)	N(1)−Cu(1)−P(2)	120.84(6)
Cu(1)−P(1)	2.2683(8)	N(2)−Cu(1)−P(1)	104.91(6)
		N(1)−Cu(1)−P(1)	112.12(6)
		P(2)−Cu(1)−P(1)	113.35(3)
		Compound **4**	
Cu(1)−N(3)	2.016(3)	N(3)−Cu(1)−N(2)	78.72(12)
Cu(1)−N(2)	2.150(3)	N(3)−Cu(1)−P(1)	124.91(9)
Cu(1)−P(1)	2.2310(11)	N(2)−Cu(1)−P(1)	111.80(9)
Cu(1)−P(2)	2.2386(10)	N(3)−Cu(1)−P(2)	125.91(9)
		N(2)−Cu(1)−P(2)	109.19(9)
		P(1)−Cu(1)−P(2)	102.24(4)

mmol), cesium carbonate (2.00 g, 6.15 mmol), and 1,10-phenanthroline (0.110 g, 0.61 mmol) was refuxed in 2 mL of dimethyl formamide for 30 h. The product was purified by column chromatography (THF/hexanes/methanol, 1:1:0.05) and subsequent recrystalization from methylene chloride and hexanes (yield 78%). ^{1}H NMR in CD_2Cl_2 (δ, ppm, 298 K): 8.36 (bd, J = 4.2 Hz, 1H), 8.21 (d, J = 8.1 Hz, 1H), 7.89−7.80 (m, 2H), 7.56−7.45 (m, 3H), 7.40−7.26 (m, 6H). Anal. Calcd for $C_{18}H_{13}N_3$: C, 79.68; H, 4.83; N, 15.49. Found: C, 80.00; H, 4.87; N, 15.38.

Synthesis of [Cu(pbb)(PPh$_3$)$_2$][BF$_4$] (1). To a solution of pbb (28 mg, 0.10 mmol) in CH_2Cl_2 (ca. 5 mL) was added a solution of $[Cu(CH_3CN)_2(PPh_3)_2][BF_4]$ (72 mg, 10 mmol) in CH_2Cl_2 (ca. 5 mL). The yellow solution was layered with toluene (ca. 2 mL) and hexanes (ca. 2 mL). Diffusion of the layers and slow evaporation of the solvents afforded complex **1** after 1 week in 63% yield. ^{1}H NMR in CD_2Cl_2 (δ, ppm, 298 K): 8.38 (d, J = 4.80 Hz, 1H), 7.81−7.75 (m, 3H), 7.67 (d, J = 9.30 Hz, 1H), 7.44−7.32 (m, 12H), 7.27−7.20 (m, 24H), 7.01 (d, J = 8.10 Hz, 2H). ^{31}P{^{1}H} NMR in CD_2Cl_2 (δ, ppm, 298 K): 3.07. Anal. Calcd for $C_{54}H_{43}BCuF_4N_3P_2{\cdot}0.25CH_2Cl_2$: C, 67.42; H, 4.45; N, 4.35. Found: C, 67.28; H, 4.58; N, 4.55.

Synthesis of [Cu(pbb)(dppe)][BF$_4$] (2). A solution of $[Cu(CH_3CN)_4][BF_4]$ (82 mg, 0.26 mmol) and 1,2-bis(diphenylphosphenyl)ethane (dppe) (60 mg, 0.15 mmol) in CH_2Cl_2 (ca. 5 mL) was stirred for 1.5 h. A solution of pbb (45 mg, 0.16 mmol) in CH_2Cl_2 (ca. 3 mL) was added, and the mixture was stirred for 1 h to obtain a dark yellow solution. The yellow solution was layered with toluene (ca. 2 mL). Diffusion of the layers and slow evaporation of the solvents afforded complex **2** after 3 days in 88% yield. ^{1}H NMR in CD_2Cl_2 (δ, ppm, 298 K): 8.32 (d, J = 4.80 Hz, 1H), 7.84 (d, J = 4.20 Hz, 3H), 7.79 (d, J = 8.10 Hz, 1H), 7.67−7.65 (m, 2H), 7.50−7.42 (m, 12H), 7.39−7.34 (m, 10H), 7.30 (d, J = 5.40 Hz, 2H), 7.23 (d, J = 7.80 Hz, 2H), 2.76 (t, J = 6.00 Hz, 4H). ^{31}P{^{1}H} NMR in CD_2Cl_2 (δ, ppm, 298 K): −4.26. Anal. Calcd for $C_{44}H_{37}BCuF_4N_3P_2/0.25CH_2Cl_2$: C, 63.17; H, 4.46; N, 4.99. Found: C, 63.18; H, 4.48; N, 5.04.

Synthesis of [Cu(pbb)(DPEphos)][BF$_4$] (3). A solution of $[Cu(CH_3CN)_4][BF_4]$ (125 mg, 0.40 mmol) and bis[2-(diphenylphos-

(8) Frisch, M. J.; Trucks, G. W.; Schlegel, H. B.; Scuseria, G. E.; Robb, M. A.; Cheeseman, J. R.; Montgomery, J. A., Jr.; Vreven, T.; Kudin, K. N.; Burant, J. C.; Millam, J. M.; Iyengar, S. S.; Tomasi, J.; Barone, V.; Mennucci, B.; Cossi, M.; Scalmani, G.; Rega, N.; Petersson, G. A.; Nakatsuji, H.; Hada, M.; Ehara, M.; Toyota, K.; Fukuda, R.; Hasegawa, J.; Ishida, M.; Nakajima, T.; Honda, Y.; Kitao, O.; Nakai, H.; Klene, M.; Li, X.; Knox, J. E.; Hratchian, H. P.; Cross, J. B.; Bakken, V.; Adamo, C.; Jaramillo, J.; Gomperts, R.; Stratmann, R. E.; Yazyev, O.; Austin, A. J.; Cammi, R.; Pomelli, C.; Ochterski, J. W.; Ayala, P. Y.; Morokuma, K.; Voth, G. A.; Salvador, P.; Dannenberg, J. J.; Zakrzewski, V. G.; Dapprich, S.; Daniels, A. D.; Strain, M. C.; Farkas, O.; Malick, D. K.; Rabuck, A. D.; Raghavachari, K.; Foresman, J. B.; Ortiz, J. V.; Cui, Q.; Baboul, A. G.; Clifford, S.; Cioslowski, J.; Stefanov, B. B.; Liu, G.; Liashenko, A.; Piskorz, P.; Komaromi, I.; Martin, R. L.; Fox, D. J.; Keith, T.; Al-Laham, M. A.; Peng, C. Y.; Nanayakkara, A.; Challacombe, M.; Gill, P. M. W.; Johnson, B.; Chen, W.; Wong, M. W.; Gonzalez, C.; Pople, J. A. *Gaussian 03*, revision A.9; Gaussian, Inc.: Pittsburgh, PA, 2004.

phino)phenyl]ether (DPEphos) (215 mg, 0.40 mmol) in CH_2Cl_2 (ca. 5 mL) was stirred for 1.5 h. A solution of pbb (86 mg, 0.32 mmol) in CH_2Cl_2 (ca. 3 mL) was added, and the mixture was stirred for 1 h to obtain a dark yellow solution. The yellow solution was layered with toluene (ca. 2 mL) and hexanes (ca. 2 mL). Diffusion of the layers and slow evaporation of the solvents afforded complex **3** after 3 days in 60% yield. ^{1}H NMR in CD_2Cl_2 (δ, ppm, 298 K): 8.36 (d, J = 4.80 Hz, 1H), 7.79 (dd, J = 5.10, 1.80 Hz, 3H), 7.61 (t, J = 7.95 Hz, 2H), 7.51 (d, J = 8.40 Hz, 1H), 7.46−7.43 (m, 2H), 7.38−7.31 (m, 7H), 7.28−7.14 (m, 15H), 7.09−6.99 (m, 8H), 6.97−6.90 (m, 2H). ^{31}P{^{1}H} NMR in CD_2Cl_2 (δ, ppm, 298 K): −10.56. Anal. Calcd for $C_{54}H_{41}BCuF_4N_3OP_2$: C, 67.54; H, 4.30; N, 4.38. Found: C, 67.50; H, 4.21; N, 4.26.

Synthesis of [Cu(pbb)(DPPMB)][BF$_4$] (4). A solution of $[Cu(CH_3CN)_4][BF_4]$ (36 mg, 0.11 mmol) and bis(diphenylphosphinomethyl)diphenyl borate ligand {$[Ph_2B(CH_2PPh_2)_2][ASN]$, DPPMB] (66 mg, 0.10 mmol) in CH_2Cl_2 (ca. 5 mL) was stirred for 2 h. A solution of pbb (32 mg, 0.12 mmol) in CH_2Cl_2 (ca. 3 mL) was added, and the mixture was stirred for 1 h to obtain a deep red solution. The red solution was layered with toluene (ca. 2 mL) and hexanes (ca. 2 mL). Diffusion of the layers and slow evaporation of the solvents afforded complex **4** after 1 week in 72% yield. ^{1}H NMR in CD_2Cl_2 (δ, ppm, 298 K): 7.75 (t, J = 3.15 Hz, 3H), 7.57−7.54 (m, 2H), 7.49 (d, J = 7.80 Hz, 2H), 7.39−7.25 (m, 10H), 7.17−7.12 (m, 10H), 7.10−6.96 (m, 10H), 6.90−6.89 (m, 5H), 6.67 (d, J = 8.70 Hz, 1H), 2.14 (d, J = 9.90 Hz, 4H). ^{31}P{^{1}H} NMR in CD_2Cl_2 (δ, ppm, 298 K): −4.00. Anal. Calcd for $C_{56}H_{47}BCuN_3P_2\cdot 0.5CH_2Cl_2$: C, 73.42; H, 5.10; N, 4.47. Found: C, 72.85; H, 5.23; N, 4.63.

Quantum Yield Measurements. The absolute photoluminescent quantum yields of Cu(I) complexes **1**−**4** doped in PMMA films (20% complex/80% PMMA by weight) were measured at ambient temperature using a commercial fluorimeter in combination with an integration sphere according to the literature procedure.[9]

X-ray Crystallographic Analysis. Single crystals of compounds **1**−**4** were obtained from the mixed solvent solution of toluene/CH_2Cl_2/hexanes. Crystals were mounted on glass fibers for data collection. Data were collected on a Siemens P4 single-crystal X-ray diffractometer with a Smart CCD-1000 detector and graphite-monochromated Mo Kα radiation, operating at 50 kV and 30 mA at 298 K for **2** and at 180 K for **1**, **3**, and **4**. No significant decay was observed for any sample. Data were processed on a PC using the Bruker SHELXTL software package[10] (version 5.10) and were corrected for Lorentz and polarization effects. Compounds **1**−**3** belong to the monoclinic space groups $P2_1$, $P2_1/n$, and Cc, respectively, determined by the systematic absences and the successful solution and refinements of the structures, whereas compound **4** belongs to the triclinic space group $P\bar{1}$. Solvent molecules were located in the crystal lattices for **2** and **4**. For **2**, each molecule cocrystallizes with 0.5 CH_2Cl_2 solvent molecule. For **4**, one disordered CH_2Cl_2 and 0.5 disordered toluene solvent molecules per molecule of **4** were located and were partially resolved and refined. The BF_4 anions in all compounds were also found to display some degree of disordering and were refined successfully. One of the phenyl groups of in **4** displays rotational disordering that was modeled and refined successfully. Most non-hydrogen atoms except the disordered ones in **1**−**4** were refined anisotropically. All hydrogen atoms except those on disordered carbon atoms were calculated, and their contributions were included in structural factor calculations. The crystallographic data are reported in Table 1. Selected bond lengths and angles for complexes 1−4 are listed in Table 2.

Results and Discussion

Syntheses and Structures. The new *N*,*N*-chelate ligand, pbb, was synthesized by the reaction of 2-(2′-pyridyl)-benzimidazole with bromobenzene using a modified Ullmann condensation procedure reported recently by our group where CuI and 1,10-phenanthroline were used as the catalysts and Cs_2CO_3 was used as the base.[4] pbb was fully characterized by NMR spectroscopy and elemental analysis. Four different ancillary phosphine ligands, namely, PPh_3, dppe, DPEphos, and DPPMB, were used in our investigation. The bidentate chelate phosphine ligands DPEphos and DPPMB were synthesized by the procedures in refs 6 and 7. The choice of the three bidentate chelate phosphine ligands was based on the following considerations. First, the chelate phosphine ligands are known to provide better stability to the Cu(I) complex than the monodentate PPh_3 ligand.[1] Second, these three chelate phosphine ligands have distinct steric and electronic properties that offer an opportunity to examine the steric and electronic impacts of phosphine donors on the properties of the copper complexes. Third, it was shown previously that chelate phosphine ligands such as DPEphos can minimize emission quenching induced by solvent molecules or self-quenching, thus enhancing emission efficiency.[1,3] The anionic ligand DPPMB is unique among the four phosphine ligands that we studied because it allows the synthesis of a neutral Cu(I) complex instead of a salt, which is highly desirable if the Cu(I) complex were to be incorporated into OLEDs by a vacuum deposition process. Furthermore, the negatively charged ligand DPPMB might enhance the electron density on the metal center, thus having a significant impact on the MLCT state. In fact, the DPPMB ligand has been used successfully in a number of transition metal complexes including Pt(II) and Cu(I), as reported by Peters and co-workers.[6,11]

Complex **1** was obtained by the reaction of $[Cu(CH_3CN)_2(PPh_3)_2][BF_4]$ with 1 equiv of pbb under air. The syntheses of the Cu(I) complexes **2**−**4** were achieved by the reaction of $[Cu(CH_3CN)_4][BF_4]$ with pbb and the corresponding chelate phosphine ligand in a 1:1:1 ratio under a nitrogen atmosphere. Compounds **1**−**3** have a yellow color and are stable in solution and in the solid state upon exposure to air. Compound **4** has a distinct red color and decomposes gradually when exposed to air. The new complexes were fully characterized by NMR, elemental, and X-ray diffraction analyses.

The ^{31}P{^{1}H} NMR spectra for all four complexes were recorded and show that there is a considerable change in the ^{31}P chemical shifts for the four phosphine ligands in the complexes compared to those in the corresponding free ligands. Complex **1** has a chemical shift at 3.07 ppm, which is in agreement with the values observed in polynuclear Cu(I) complexes that contain the PPh_3 ligand.[4] The dppe complex

(9) (a) Plsson, L.-O.; Monkman, A. P. *Adv. Mater*. **2002**, *14*, 757. (b) Mello, J. C.; Wittmann, H. F.; Friend, R. H. *Adv. Mater*. **1997**, *9*, 230.

(10) *SHELXTL NT Crystal Structure Analysis Package*, version 5.10; Bruker Analytical X-ray Systems: Madison, WI, 1999.

(11) Thomas, J. C.; Peters, J. C. *Polyhedron* **2004**, 23, 2901.

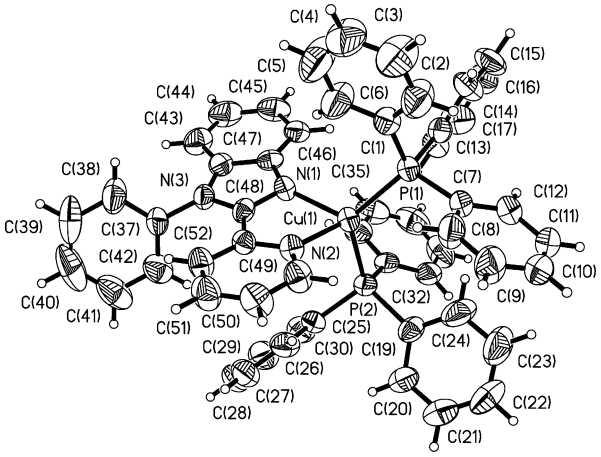

Figure 1. Structure of 1 with thermal ellipsoids and labeling schemes. The BF_4^- anion is omitted.

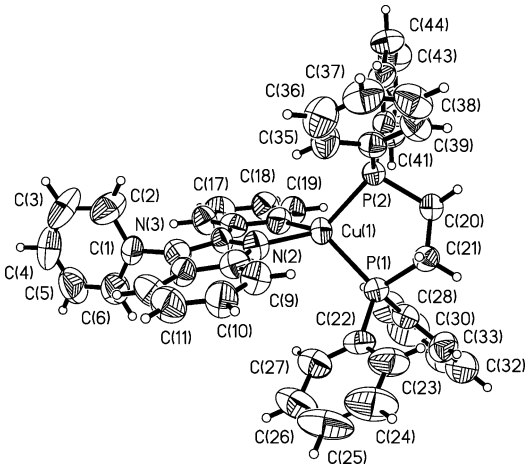

Figure 2. Structure of 2 with thermal ellipsoids and labeling schemes. The BF_4^- anion is omitted.

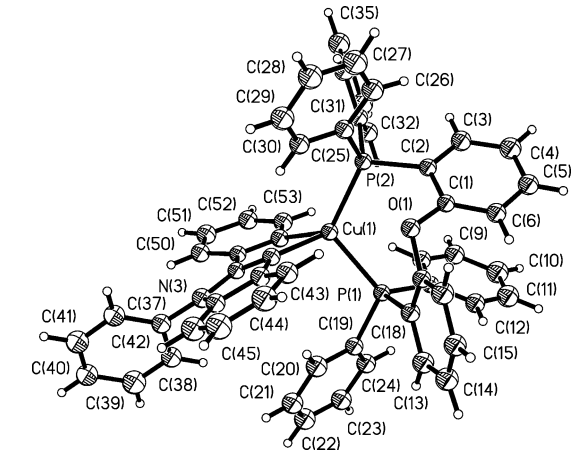

Figure 3. Structure of 3 with thermal ellipsoids and labeling schemes. The BF_4^- anion is omitted.

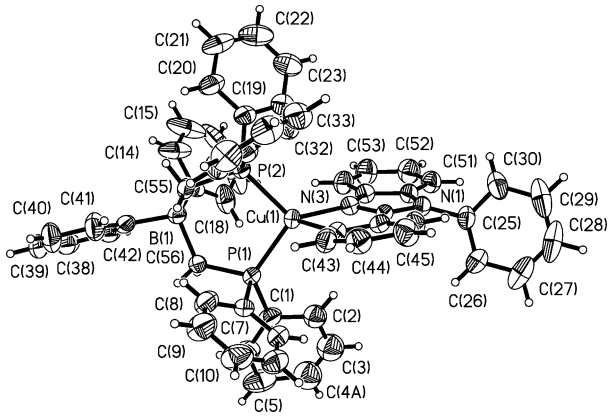

Figure 4. Structure of 4 with thermal ellipsoids and labeling schemes. For the disordered phenyl ring, only one set of the disordered atoms [C(2A) and C(3A)] are shown.

2 and the DPEphos complex **3** have ^{31}P chemical shifts at −4.26 and −10.56 ppm, respectively, which are comparable to those of previously reported Cu(I) DPEphos and Cu(I) dppe complexes.[7,12] For complex **4**, the ^{31}P chemical shift appears at −4.00 ppm, which is within the normal expected range for the DPPMB ligand.[6,11]

The crystal structures of the Cu(I) complexes **1**−**4** are shown in Figures 1−4, respectively. For complexes 1−3, the BF_4^- anion is omitted for clarity. The Cu(I) center in all four complexes has a distorted tetrahedral geometry. The dihedral angles between the N−Cu−N plane and the P−Cu−P plane for the four complexes are 90.2°, 81.9°, 94.4°, and 86.8°, respectively. The Cu−N (pyridyl) bond lengths for the pyridyl bond [avg 2.119(4) Å] are greater than the Cu−N (imidazolyl) bond lengths [avg 2.042(4) Å], indicating a stronger bond for the imidazolyl nitrogen, consistent with previously reported polynuclear Cu(I) complexes containing the 2-(2′-pyridyl)benzimidazolyl group.[4] The Cu−N bond lengths observed in **1**−**4** are comparable to those in $[Cu(phen)(PPh_3)_2]NO_3$ (2.075 Å) and $[Cu(dmp)(PPh_3)_2]NO_3$ (2.117 Å).[13] The Cu−P bond lengths for all four complexes are similar. The N−Cu−N bond angles are similar for complexes **1**, **3**, and **4** (78.6−78.8°) with little variation. The N−Cu−N bond angle of **2** is somewhat greater, 80.1°, clearly due to the reduced steric congestion. In contrast, however, the P−Cu−P angles vary dramatically from 92.02(6)° for complex **2** to 124.12(6)° for complex **1** as shown in Table 2. Previously, it was observed that the P−Cu−P angle is 115.85(9)° for $[Cu(phen)(PPh_3)_2]NO_3$ and 122.7(1)° for the more sterically crowded complex $[Cu(dmp)(PPh_3)_2]NO_3$; the latter is similar to that of **1**.[13] The P−Cu−P bite angle of **1** is also similar to those observed in polynuclear Cu(I) complexes that contain PPh_3 ligands with a similar coordination environment.[4] The fact that the dppe complex **2** has the smallest P−Cu−P angle is an indication that the dppe ligand is the least crowded. The DPEphos natural bite angle was calculated by Kranenburg et al. to be 102.2°, with a flexibility range from 86° to 120°.[7] $[Cu(dmp)(DPEphos)]^+$ has a P−Cu−P angle[1] of 116.44°, which is slightly larger than that found in complex **3** (113.35°). One notable feature of the *N*,*N*-chelate ligand pbb in complexes **1**−**4** is that the phenyl ring and the 2-(2′-pyridyl)benzimidazolyl unit in pbb are not coplanar, but have a dihedral angle of 67.5°, 84.1°, 62.4°, and 65.5°, respectively, which is clearly caused by the nonbonding interactions between the ortho hydrogen atoms of the phenyl ring and the pyridyl ring. Similar

(12) Tolman, C. A. *Chem. Rev.* **1977**, *77*, 319.
(13) Kirchhoff, J. R.; McMillin, D. R.; Robinson, W. R.; Powell, D. R.; McKenzie, A. T.; Chen, S. *Inorg. Chem*. **1985**, *24*, 3928.

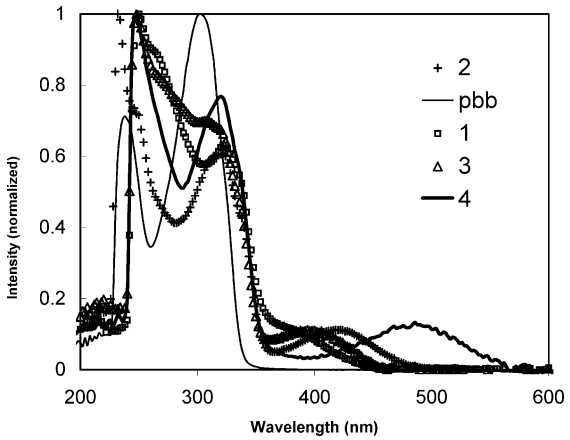

Figure 5. UV−vis spectra of pbb and complexes 1−4 in CH_2Cl_2 ([C] ≈ 10^{-5} M).

phenomena have also been observed in other 2-(2′-pyridyl)-benzimidazolyl derivative ligands with an aromatic linker.[4] The oxygen atom of the DPEphos ligand in **3** is at a distance of 3.16 Å from the Cu(1) center and opposite that of N(1) [N(1)−Cu(1)−O(1) = 176.8°]. Similar Cu−O separations have also been reported in DPEphos Cu(I) complexes that contain 1,10-phenanthroline and derivative ligands.[1]

Spectroscopic and Electrochemical Properties. In CH_2Cl_2, the free ligand shows two absorption peaks at $\lambda_{max} \approx 240$ and 300 nm attributed to a $\pi \rightarrow \pi^*$ transition centered on the 2-(2′-pyridyl)benzimidazolyl. As shown in Figure 5 and Table 3, in CH_2Cl_2, complexes 1−4 have multiple absorption peaks in the 200−320 nm region that can be attributed to both pbb and phosphine ligands. In addition, a low-energy and broad absorption band is observed for all complexes, which is characteristic of metal-to-ligand charge-transfer (MLCT) transitions. For complex **1**, this MLCT absorption band appears at $\lambda_{max} = 370$ nm, which is similar to the values observed in polynuclear Cu(I) complexes involving 2-(2′-pyridyl)benzimidazolyl functionalized ligands and PPh_3.[4] For complexes **2**−**4**, this MLCT band shifts to lower energy with $\lambda_{max} \approx 420$ nm for **2**, 400 nm for **3**, and 485 nm for **4**. This dramatic variation of the MLCT band supports the conclusion that the ancillary phosphine ligands significantly perturb the MLCT state of the copper complexes. The trend of the MLCT band observed for complexes **1**−**3** is consistent with that observed for the $[Cu(Phen)(P)_2]^+$ and $[Cu(dmp)(P)_2]^+$ complexes where $(P)_2 = 2PPh_3$, dppe, and DPEphos.[1] The energy of the MLCT band of **4** is dramatically lower than those of **1**−**3**, which is clearly responsible for the distinct red color of complex **4**. The optical band gap using the edge of the lowest-energy absorption band was determined to be 2.80, 2.50, 2.60, and 2.10 eV for complexes **1**−**4**, respectively. Sakaki et al. reported a series of $[Cu(dmp)L_2]^+$ complexes with $L = PPh_n(C_6H_4OMe\text{-}p)_{3-n}$ where the phosphine ligands have a similar cone angle but different electron-donating capabilities because of the variation in the number of methoxy-substituted phenyl groups.[14] It was observed that the MLCT band of the $[Cu(dmp)L_2]^+$ complex shifts to somewhat longer wavelengths with increasing electron-donating character of the phosphine.[14] Therefore, judging from the MLCT energy, the electron-donating capabilities of the ancillary phosphine ligands appear to increase in the order DPPMB > dppe > DPEphos > PPh_3. It is not surprising that the anionic ligand DPPMB in **4** is the strongest electron donor, as a formally negative charge on the ligand is anticipated to increase the electron density on the metal center.[6] It has been noted by McMillin and co-workers that a wider P−Cu−P bite angle can decrease the dσ^* interactions and enhance the energy required for MLCT excitation.[1] The P−Cu−P angle, therefore, might also play a role in the observed band gap variation of compounds **1**−**4**. In fact, the P−Cu−P bond angles of **1**−**3** follow the order of **1** (124.12°) > **3** (113.35°) > **2** (92.02°), which is the same order as the MLCT energies (372, 396, and 422 nm, respectively), consistent with the observations of McMillin et al. We can therefore conclude that, for complexes **1**−**3**, steric factors play a key role in the electronic properties of the complex. However, for complex **4**, which has a P−Cu−P bond angle (102.24°) much greater than that of **2** but an MLCT energy

Table 3. Absorption and Emission Data

	absorption[a]	Em, λ_{max} (λ_{EX}) nm				τ (μs)	
compd	λ_{max}, nm (ϵ, M^{-1} cm^{-1})	in DCM[a] 77 K	in PMMA[b] 77 K	in PMMA[b] room temp	ϕ[c]	in DCM 77 K	in PMMA 77 K
1	236 (34600) 248 (28034) 324 (16991) 372 (3452)	553	561	536	13	296(6), 115(5)	353(1)
2	232 (36028) 246 (26503) 318 (21854) 422 (4049)	586	597	545	<1%	291(8), 106(4)	503(6) 136(3)
3	236 (34916) 246 (29064) 318 (21565) 396 (4014)	564	557	537	1.04	247(6), 106(6)	322(4), 122(3)
4	236 (32908) 316 (16507) 484 (1579)	587	603	593	<1%	315(3), 111(3)	228.8(7)
pbb	238 (12741) 302 (17893)	382	380	394		311(2)[d]	

[a] [c] ≈ 10^{-5} M. [b] 20 wt % in PMMA. [c] 20 wt % in PMMA, room temperature. [d] For the phosphorescent band with $\lambda_{max} = 525$ nm obtained by using a time-resolved phosphorescent spectrometer.

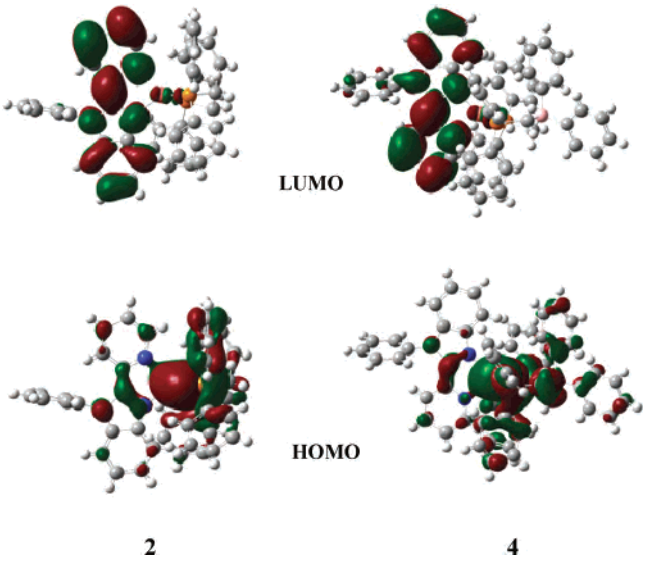

Figure 6. HOMO and LUMO diagrams for compounds **2** and **4**.

(484 nm) much less than that of **2**, electronic factors clearly dominate. The MLCT bands of **1**−**4** shift somewhat toward shorter wavelengths in polar solvents such as CH_3OH and DMF (see Supporting Information), which is consistent with the behavior of Cu(I) phenanthroline complexes and the polynuclear Cu(I) 2-(2′-pyridyl)benzimidazolyl derivative complexes.[1,4]

In CH_3CN solution, complexes **1**−**3** display an irreversible oxidation peak with peak heights at ∼1.80 V (**1**), 1.50 V (**2**), 1.60 V (**3**), and 0.60 V (**4**), which can be attributed to the oxidation of Cu(I) to Cu(II). The exceptionally low oxidation potential displayed by compound **4** indicates that it has a relatively high HOMO level, which is most likely due to the presence of the anionic DPPMB chelate ligand, which increases the electron density on the copper center, thus destabilizing the HOMO level. The first reduction peaks for the four complexes were observed at −1.52 V (**1**), −1.60 V (**2**), −1.60 V (**3**), and −1.75 V (**4**), which are attributed to the reduction of the *N*,*N*-chelate ligand. Using the reduction and oxidation potentials, the electrochemical band gaps for complexes **1**−**4** were estimated to be 3.36, 3.10, 3.20, and 2.35 eV, respectively. Although the values of the electrochemical band gaps deviate considerably from those of the optical band gaps, the general trends revealed by the electrochemical and optical band gaps are consistent: compound **1** has the largest and compound **4** the smallest HOMO−LUMO energy gap.

Ab Initio MO Calculations. To further understand the variation of the electronic properties of compounds **1**−**4**, ab initio molecular orbital calculations were performed for all four complexes using the Gaussian suite of programs (Gaussian 03) and geometric parameters obtained from single-crystal X-ray diffraction analysis.[8] The molecular orbital surfaces generated by Gaussian 03 for all four molecules show that the HOMO is indeed dominated by the d orbital of the copper(I) ion, but significant contributions from the phosphine ligands and a small contribution from the pbb ligand are also evident. The LUMO is almost entirely made up of atomic orbitals of the pbb ligand. (The LUMO and HOMO diagrams for compounds **2** and **4** are shown in Figure 6, as representative examples.) Thus, the MO calculation results confirmed that the lowest electronic transition in complexes 1−4 is indeed MLCT in nature, but with considerable contribution from the phosphine ligands (i.e., phosphine ligand to pbb charge transfer). The HOMO and LUMO energies, the band gaps, and the optical and electrochemical band gaps are summarized in Table 4. As shown in Table 4, the variations among complexes 1−3 in both the HOMO energy (from −0.29424 to −2.8628 Hartree) and the LUMO energy (from −0.17577 to −0.16716 Hartree) are small. In contrast, the HOMO (−0.18349 Hartree) and LUMO (−0.09006 Hartree) energy levels of complex **4** are substantially higher than those of **1**−**3**. The HOMO−LUMO band gaps obtained from Gaussian 03 MO calculations were 3.37, 3.01, 3.28, and 2.54 eV, respectively, for complexes **1**−**4**. The band gap trend obtained from the MO calculations is consistent with the electrochemical and UV−vis data. The MO results support the conclusion that the anionic DPPMB ligand destabilizes both the HOMO and the LUMO levels in complex **4** by increasing the electron density on the metal center. However, because the destabilization of the HOMO level is much more pronounced than that of the LUMO level, the net result is an overall decrease of the band gap in **4** compared to those in **1**−**3**.

Luminescent Properties. The free ligand pbb emits a purple color when irradiated with UV light with $\lambda_{max} \approx 380$ nm at room temperature in CH_2Cl_2, which is attributed to the fluorescent emission of the singlet state. In contrast, complexes **1**−**4** all emit in the yellow-orange region with a broad emission band and λ_{max} at ∼553, 586, 564, and 587 nm, respectively, at 77 K in CH_2Cl_2 when excited by the MLCT energy. At ambient temperature, complexes **1**−**4** do not display any detectable emission in solution. The emission energy appears to follow the same trend as the absorption energy, with complex **1** having the highest emission energy. The exception is complex **2**, which has an emission energy similar to that of **4** in solution. This anomaly could be attributed to the fact that **2** is the least sterically crowded molecule, and hence the most susceptible to structural

Table 4. HOMO and LUMO Energies and Bandgaps

	MO data			experimental data			
complex	HOMO (Hartree)	LUMO (Hartree)	gap (eV)	optical band gap (eV)	E_{ox} (V)	E_{red} (V)	electrochemical band gap (eV)
1	−0.29424	−0.17036	3.37	2.79	1.80	−1.52	3.32
2	−0.28628	−0.17577	3.01	2.50	1.50	−1.60	3.10
3	−0.28777	−0.16716	3.28	2.58	1.60	−1.60	3.20
4	−0.18349	−0.09006	2.54	2.10	0.60	−1.75	2.35

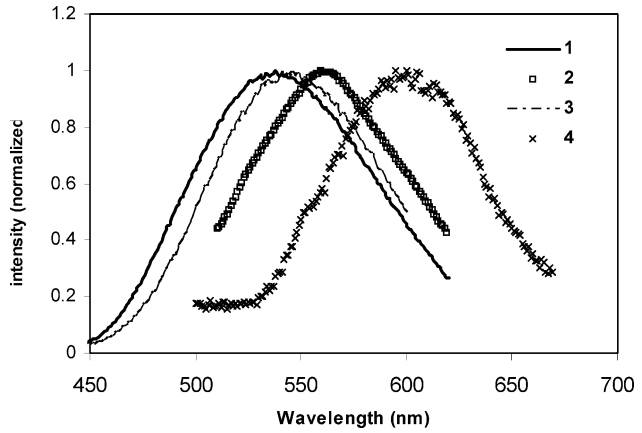

Figure 7. Emission spectra of 1−4 in PMMA films (20 wt %) at ambient temperature.

relaxation, resulting in a relatively low emission energy in solution.[15] The emission bands of **1**−**4** shift toward shorter wavelength in polar solvents such as DMF. For example, the emission wavelength of **3** in CH_2Cl_2 is at 564 nm, which shifts to 540 nm in DMF. Interestingly, however, in THF, which is a slightly less polar solvent than CH_2Cl_2, the emission band of **3** also shifts to a shorter wavelength, 544 nm. The polarity of the solvent molecules appears not to be the only factor that is responsible for the emission energy shift. Although complexes **1**−**4** are not emissive in solution at ambient temperature, they do emit when doped into PMMA polymer as shown by Figure 7. The emission peak in PMMA at ambient temperature is considerably blue shifted, compared to that at 77 K, which can be attributed to the increased contribution of emission from the singlet MLCT state and the pbb ligand's triplet emission (λ_{max} = 525 nm) at ambient temperature. The emission data for complexes 1−4 are provided in Table 3. Complex **4** is unique because it is a charge-neutral molecule and consistently displays a red-orange emission color in solution and in PMMA. Compounds **1**−**4** do not emit as pure solids at ambient temperature. The emission spectra of **1**−**4** as pure solids at 77 K are similar to those in PMMA matrix. The decay lifetimes at 77 K in frozen solution or in PMMA matrix were determined for all four complexes by using a time-resolved phosphorescence spectrometer. When fitted with a single decay component, some deviation from the experimental data was observed for most of the complexes. As a result, two components were used in fitting the decay curve, producing a good fit. As shown in Table 3, complexes **1**−**4** display remarkably long decay lifetimes (the longer lifetime is the dominating component for all complexes), which are similar to those observed for the polynuclear Cu(I) complexes that contain the 2-(2′-pyridyl)benzimidazolyl group and the PPh_3 ancillary ligand that we reported recently.[4] These long decay lifetimes confirmed that the observed MLCT emission is from the triplet state. The variation of the phosphine ligands appears to have no dramatic impact on the decay lifetime. The long decay lifetimes of **1**−**4** are in sharp contrast to those of Cu(I) complexes of phenanthroline and derivative ligands, which were reported to have much shorter times (<50 μs).[1,3] It is likely that the partial involvement of the phosphine ligands in the charge-transfer process that leads to a partial ligand-to-ligand charge-transfer character in the lowest electronic transition might play a role in the exceptionally long decay lifetimes of **1**−**4**. The lack of emission by complexes **1**−**4** in solution at ambient temperature could be explained by their long decay lifetimes, which make them highly susceptible to solvent-induced thermal quenching. Attempts were made to measure the quantum yields of complexes **1**−**4** in PMMA by using integration sphere methods. The quantum yields of complexes **1**−**4** are included in Table 3. Unlike the Cu(I) phen or dmp complexes where the chelate phosphine ligands such as DPEphos were found to increase quantum efficiency, compared to PPh_3,[1,3] our DPEphos complex **3** has a much lower quantum efficiency.

Mononuclear Complex versus Dinuclear Complex. The coordination environment of complex **1** is essentially identical to that of the dinuclear complex[4] $[Cu_2(bmbp)(PPh_3)_4][BF_4]_2$ shown in Chart 1. In fact, compound **1** can be considered as one-half of the dinuclear Cu(I) compound. Hence, compound **1** and the dinuclear compound $[Cu_2(bmbp)(PPh_3)_4][BF_4]_2$ provide an opportunity to compare the difference between mononuclear copper(I) complexes and the corresponding dinuclear copper(I) complexes. In terms of emission energy, there is very little difference between **1** and the dinuclear compound. In addition, the two compounds have similar emission quantum efficiencies {13% for **1** and 15% for $[Cu_2(bmbp)(PPh_3)_4][BF_4]_2$} in PMMA. This is not entirely surprising, as we have shown that there is no evidence for electronic communication between the two Cu(I) centers in $[Cu_2(bmbp)(PPh_3)_4][BF_4]_2$, which is mostly due to the orthogonal arrangement between the central biphenyl unit and the 2-(2′-pyridyl)benzimidazolyl chelating groups. The major difference between **1** and $[Cu_2(bmbp)(PPh_3)_4][BF_4]_2$ is the decay lifetime: at 77 K, the mononuclear compound **1** has a decay lifetime (the dominant slow component) about 80 μs longer in CH_2Cl_2 and about 160 μs longer in PMMA than those of $[Cu_2(bmbp)(PPh_3)_4][BF_4]_2$. Clearly, the presence of the extra copper(I) center in the dinuclear complex does appear to shorten the decay lifetime considerably, despite the fact that the two Cu(I) centers are far from each other (17.32 Å).[4]

Concluding Remarks

Our investigation of the four new Cu(I) complexes based on the pbb chromophore and four different ancillary phosphine ligands leads to the following conclusions: (1) Sterically, the dppe ligand is the least demanding and PPh_3 is the most demanding, which results in considerable variations in P−Cu−P bond angles in the four complexes, but little impact on Cu−P and Cu−N bond lengths and the N−Cu−N bond angles. (2) Both steric and electronic properties of the phosphine ligands have an impact on the electronic properties of the copper complexes. For the neutral

(14) Sakaki, S.; Mizutani, H.; Kase, Y.-I.; Inokuchi, K.-J.; Arai, t.; Hamada, T.. *J. Chem. Soc., Dalton Trans.* **1996**, 1909.
(15) Eggleston, M. K.; McMillin, D. R.; Koenig, K. S.; Pallenberg, A. J. *Inorg. Chem.* **1997**, *36*, 172.

phosphine ligands PPh_3, DPEphos, and dppe, steric factors appear to play a key role in the variation of the electronic properties of complexes 1−3. In contrast, for the anionic ligand DPPMB, electronic factors appear to be dominant, which results in complex **4** having the smallest HOMO−LUMO energy gap. (3) All four complexes display characteristic MLCT emissions with significant contributions from the phosphine ligands, which is clearly phosphorescent in nature, as evidenced by their exceptionally long decay lifetimes. The long decay lifetimes might hinder the use of the new complexes as phosphorescent emitters in OLEDs, but might be very desirable for using these molecules in photochemistry. (4) Among complexes **1**−**4**, **4** is a unique molecule because it displays a red color and is a neutral molecule. In principle, compound **4** could be incorporated into OLEDs by a vacuum deposition process. However, its poor stability along with the long decay lifetime preclude its use in OLEDs. (5) The mononuclear Cu(I) complex **1** does not show a significant difference in terms of electronic properties from the corresponding dinuclear complex. For the 2(2′-pyridyl)benzimidazolyl-based complexes, for applications in OLEDs, the polynuclear Cu(I) complexes are more attractive because of their considerably shorter decay lifetimes, whereas for photochemical applications, the mononuclear complexes might be better because of their long decay lifetimes. (6) The impact of the phosphine ligands, PPh_3, dppe, and DPEphos, on the electronic properties of the 2-(2′-pyridyl)benzimidazolyl-based Cu(I) complexes is parallel to that observed for the phenanthroline-based Cu(I) complexes. The major difference between the two systems is the decay lifetime: the 2-(2′-pyridyl)benzimidazolyl-based complexes have a much longer decay lifetime than the phen-based Cu(I) complexes. The participation of the phosphine ligands in the charge-transfer process might be partially responsible for the observed long decay lifetimes of complexes **1**−**4**. Furthermore, unlike the phenanthroline-based Cu(I) complexes, where the chelate phosphine ligands such as DPEphos are known to substantially increase the emission quantum efficiency, compared to the PPh_3 ligand, the chelate phosphine ligands for the 2-(2′-pyridyl)benzimidazolyl-based Cu(I) complexes appear to dramatically decrease the emission quantum efficiency.

Acknowledgment. We than the Natural Sciences and Engineering Research Council of Canada for financial support. We are indebted to Dr. Jian-Ping Lu at the National Research Council for his assistance in recording the quantum yields of the copper complexes.

Supporting Information Available: Emission spectra of complexes **1**−**4** in CH_2Cl_2 at 77 K, complete X-ray diffraction data for **1**−**4**, including tables of atomic coordinates, thermal parameters, bond lengths and angles, and hydrogen parameters. This material is available free of charge via the Internet at http://pubs.acs.org.

IC051412H